Spontaneous Polymer Thin Film Assembly and Organization Using Mutually Immiscible Side Chains

F. Sun,[||] D. G. Castner,[‡] G. Mao,[†] W. Wang,[†] P. McKeown,[§] and D. W. Grainger*[,†]

Contribution from the Department of Chemistry, Colorado State University, Fort Collins, Colorado 80523-1872, National ESCA and Surface Analysis Center for Biomedical Problems and Department of Chemical Engineering, University of Washington, Seattle, Washington 98195, Physical Electronics Inc., 6509 Flying Cloud Drive, Eden Prairie, Minnesota 55344

Received July 6, 1995[⊗]

Abstract: Polymer ultrathin film self-assembly and organization on solid substrates has been directed using grafted siloxane copolymers bearing mutually immiscible alkyl and perfluoroalkyl side chains. Polysiloxanes grafted with both alkyl disulfide and perfluoroalkyl side chains have been synthesized and characterized. These terpolymer systems assemble spontaneously on gold surfaces, forming bound polymeric monolayers organized by *intra*molecular phase separation. Interfacially bound polymer monolayer fabrication is driven by multipoint alkyl disulfide side chain chemisorption to gold surfaces from dilute organic solution. Immiscible perfluoroalkyl side chains of low interfacial energy enrich the ambient-exposed outer regions of these monolayers, yielding a novel bound polymer monolayer with an anisotropic, layered structure and perfluorinated surface properties. Ellipsometry indicates that these polymer films have thicknesses ranging from 22 to 32 Å, depending on solution conditions and chemistry. Angular-dependent X-ray photoelectron spectroscopy has provided a depth profile of the bound polymer films, detailing the anisotropic composition resulting from perfluoroalkyl surface enrichment. Static secondary ion mass spectrometry measurements support the enrichment of perfluoroalkyl groups in the outer atomic levels of these films. Cyclic voltammetry using the redox probes $Fe(CN)_6^{3-}$ and methylviologen with film-coated gold electrodes evaluated film-attenuated electron transfer. Time-of-flight secondary ion mass spectrometry has been used to image micropatterned polymer surfaces lithographed at high resolution both before and after organic monolayer assembly. Qualitative and quantitative information on film spatial organization and surface chemistry distribution on microstructures was obtained.

Introduction

Organization of molecules in two dimensions has long been sought as a method to provide ultrathin, durable materials with novel barrier or microstructural properties.[1] Polymerizations are commonly pursued in fabricating stable ultrathin organic films in order to increase film cohesion, durability, and functional properties.[2] Methods involving Langmuir−Blodgett (L−B) mono- and multilayers, including post-transfer-thermal polymerization[3] and photopolymerization,[2,4] electrostatic polymer adsorption,[5] and prepolymerized amphiphile assembly have been reported.[6] Self-assembly strategies using organothiols, disulfides, and alkyl silanes have also utilized *in situ* polymerization methods to stabilize interfacial order and stability.[7] Chiral recognition elements also drive monomer assembly in two dimensions and subsequently facilitate polymerization of these ordered arrays.[8] Redox-active polymers have also been synthesized, attaching to substrates via specific anchoring groups.[9] Additionally, diacetylene monomers have been anchored on gold surfaces and polymerized topochemically using photopolymerization.[10]

As an alternative, we use a strategy (Figure 1) that hybridizes the concept of prepolymerized L−B organization[6] together with organic self-assembled film architecture on solid supports.[11] Two architectural requirements are proposed for successful fabrication of prepolymerized, anchored self-assembled films: a flexible polymer backbone readily facilitating side chain rearrangements and exposed anchor groups facilitating specific interfacial binding. Multipoint attachment of soluble polymer coils by numerous anchoring polymer side chains drives an irreversible

[†] Colorado State University.
[‡] University of Washington.
[§] Physical Electronics Inc.
[||] Current address: Nalco Chemical Co., Naperville, IL 60563-1198
* Address correspondence to this author.
[⊗] Abstract published in *Advance ACS Abstracts,* February 1, 1996.

(1) Swalen, J. D.; Allara, D. L.; Andrade, J. D.; Chandross, E. A.; Garoff, S.; Israelachvilli, J.; McCarthy, T. J.; Murray, R.; Pease, R. F.; Rabolt, J. F.; Wynne, K. J.; Yu, H. *Langmuir* **1987**, *3*, 932.

(2) (a) Ringsdorf, H.; Schlarb, B.; Venzmer, J. *Angew. Chem. Int., Ed. Engl.* **1988**, *27*, 113. (b) Arslanov, V. V. *Adv. Colloid Interface Sci.* **1992**, *40*, 307.

(3) (a) Engel, A. K.; Yoden, T.; Sanui, K.; Ogata, N. *J. Am. Chem. Soc.* **1985**, *107*, 8308. (b) Kakimoto, M.; Morikawa, A.; Nishikata, Y.; Suzuki, M.; Imai, Y. *J. Colloid Interface Sci.* **1988**, *121*, 599. (c) Rabe, J. P.; Rabolt, J. F.; Brown, C. A.; Swalen, J. D. *J. Chem. Phys.* **1986**, *84*, 4096.

(4) (a) Nakanishi, F.; Okada, S.; Nakanishi, H. *Polymer* **1989**, *30*, 1959. (b) Uchida, M.; Tanizaki, T.; Oda, T.; Kajiyama, T. *Macromolecules* **1991**, *24*, 3238. (c) Akiomoto, A.; Dorn, K.; Gros, L.; Ringsdorf, H.; Schupp, H. *Angew. Chem., Int. Ed. Engl.* **1981**, *20*, 90. (d) Lopez, E.; O'Brien, D. F.; Whitesides, T. H. *J. Am. Chem. Soc.* **1982**, *104*, 305.

(5) (a) Decher, G.; Hong, J. D.; Schmitt, J. *Thin Solid Films* **1992**, *210/211*, 831. (b) Shimomura, M.; Fujii, K.; Karg, P.; Frey, W.; Sackmann, E.; Meller, P.; Ringsdorf, H. *Jpn. J. Appl. Phys.* **1988**, *27*, L1761.

(6) (a) Elbert, R.; Laschewsky, A.; Ringsdorf, H. *J. Am. Chem. Soc.* **1985**, *107*, 4134. (b) Davis, F.; Hodge, P.; Towns, C. R.; Ali-Adib, A. *Macromolecules* **1991**, *24*, 5695. (c) Biddle, M. B.; Lando, J. B.; Ringsdorf, H.; Schmidt, G.; Schneider, J. *Colloid Polym. Sci.* **1988**, *266*, 806.

(7) Li, D.; Ratner, M. A.; Marks, T. J.; Zhang, C.; Yang, J.; Wong, G. K. *J. Am. Chem. Soc.* **1990**, *112*, 7389.

(8) Stupp, S. I.; San, S.; Lin, H. C.; Li, L. S. *Science* **1993**, *259*, 59.

(9) Albagli, D.; Bazan, G. C.; Schrock, R. R.; Wrighton, M. S. *J. Am. Chem. Soc.* **1993**, *115*, 7328.

(10) (a) Batchelder, D. N.; Evans, S. D.; Freeman, T. L.; Häuβling, L.; Ringsdorf, H.; Wolfe, H. *J. Am. Chem. Soc.* **1994**, *116*, 1050. (b) Kim, T.; Crooks, R. M.; Tsen, M.; Sun, L. *J. Am. Chem. Soc.* **1995**, *117*, 3963.

(11) For a review, see: Ullman, A. *Ultrathin Films*; Academic Press: New York, 1990.

0002-7863/96/1518-1856$12.00/0

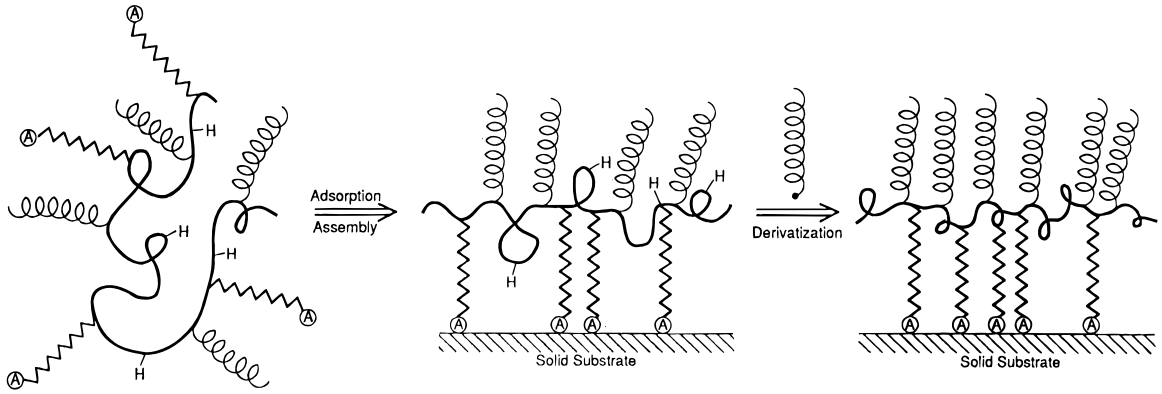

Figure 1. Conceptual representation of polymer solution coil transition to anchored two-dimensional monolayer coating. Grafted terpolymers self-organize into a three-tiered, layered structure upon interfacial binding, enriching the film's surface region with lowest energy polymer perfluorocarbon components. Functional units may be left along the polymer backbone for further in-situ derivatization and chemical modification.

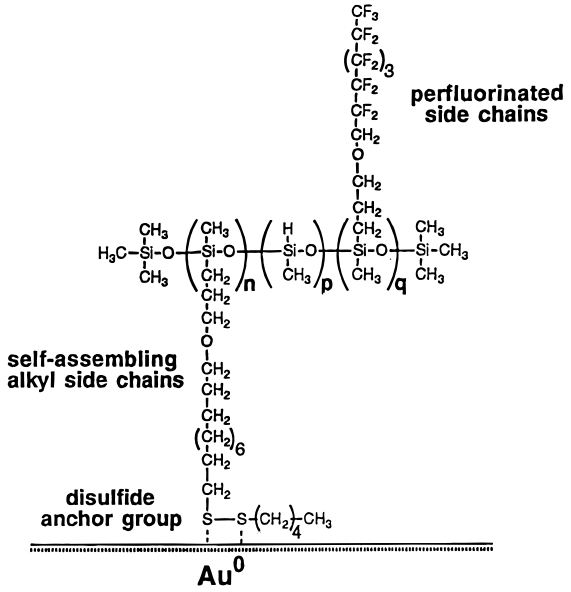

Figure 2. Chemical architecture for self-assembling polymers based on poly(methylsiloxane) main chains, perfluoroalkyl side chains, and alkyl disulfide anchoring chains.

adsorption process resulting in a tightly bound polymer monolayer. Acrylate-grafted copolymers containing alkyl disulfide or thioether anchor chains demonstrate this behavior on gold substrates,[12,13] as do siloxane oligomers bearing propyl mercaptan side chains.[14] Assemblies of these oligomers on gold create monolayers stabilized by thiolate−gold anchors. Propyl mercaptan chains left unbound and surface-exposed are readily derivatized using photoaddition reactions as schematically shown in Figure 1.[14]

We describe here a new polymer (shown in Figure 2) designed such that chemical incompatibility between bound polymer units drives organization within the anchored polymer assembly. Polysiloxanes are highly flexible, mobile polymers, exhibiting very low glass transition temperatures. These polymers also demonstrate very limited miscibility with both hydrocarbon and fluorinated compounds.[15] Because perfluorocarbon and hydrocarbon side chain components phase separate from each other[16] as well as from polysiloxane phases,[15] the copolymer architecture unfolds once bound to the solid surface. *Intra*chain immiscibility compels the siloxane backbone to position itself upon an underlying layer of chemisorbed alkyl disulfide side chains anchored on the gold surface. Lowest energy perfluoroalkyl chains remain layered above a region enriched in siloxane backbone, exposed at the ambient interface by a thermodynamic drive to minimize film interfacial tension with air.[17] The synthesis and characterization of these perfluoroalkyl-enriched polymer films using surface-sensitive and electrochemical techniques are reported.

Experimental Section

Materials. l-Octadecanethiol (98%), allyl chloride (98%), allyl alcohol (99%), *n*-pentanethiol (98%), thioacetic acid (96%), potassium ferricyanide (99+%), and tetramethylammonium hydrogen sulfate monohydrate (TAMHS) (98%) were purchased from Aldrich and used as received. 11-Bromo-1-undecene (Lancaster, 98%), pentadecafluoro-1-octanol (PCR Florida, 97%), poly(hydrogenmethylsiloxane) (PHMS) (Hüls America, average molecular weight 4750 as determined by ^{1}H-NMR in this laboratory), and platinum divinyltetramethyldisiloxane (Hüls America, 3% in xylene) were all used as supplied without further purification. Toluene (Chempure) was refluxed over sodium metal for 4−6 h and distilled prior to use. Chloroform for final polymer sample storage use was dried over P_2O_5 and then distilled. Other solvents including reagent-grade acetone (Chempure), ethyl acetate (Chempure), methylene chloride (Chempure), and ethanol (EM Science) were used as received. Chromatographically pure 4,4′-dimethylbipyridinium ion (methylviologen, MV^{2+}) was a gift from Professor J. K. Hurst (Washington State University). Water was fed from a reverse osmosis unit to a Millipore unit prior to all experiments (18 mΩ resistivity).

Polymer Synthesis. Polymers used for studies of spontaneous thin film assembly feature a flexible siloxane backbone and grafted mutually immiscible hydrocarbon and fluorocarbon side chains (Figure 2). These polymers were prepared by co-hydrosilylation of linear poly(hydrogenmethylsiloxane) (PHMS) with both side-chain-forming olefins as described in the supporting information for this article.

Synthesis of *n*-Pentadecafluorooctyl Allyl Ether (5). Compound **5** was synthesized according to a reported method[18] with minor modifications. *n*-Pentadecafluoro-1-octanol (8.50 g, 21.25 mmol) was added to a 50% caustic soda solution (60 mL) containing 0.76 g (4.0 mmol) of tetramethylammonium hydrogen sulfate (TMAHS) as a phase transfer catalyst. The mixture was vigorously stirred for 10 min. After 20.0 g (261.3 mmol) of allyl chloride was added, the mixture was stirred

(12) (a) Sun, F.; Grainger, D. W. *J. Polym. Sci. A, Polym. Chem.* **1993**, *31*, 1729. (b) Sun, F.; Grainger, D. W.; Castner, D. G. *Langmuir* **1993**, *9*, 3200. (c) Sun, F.; Grainger, D. W.; Castner, D. G.; Leach-Scampavia, D. *J. Vac. Sci. Technol.* **1994**, *12*, 2499. (d) Sun, F.; Lei, Y.; Grainger, D. W. *Colloids Surf.* **1994**, *93*, 191.

(13) Lenk, T. J.; Hallmark, V. M.; Rabolt, J. F.; Häussling, L.; Ringsdorf, H. *Macromolecules* **1993**, *26*, 1230.

(14) Sun, F.; Grainger, D. W.; Castner, D. G., Leach-Scampavia, D. *Macromolecules* **1994**, *27*, 3053.

(15) (a) Yilgor, I.; Steckle, W. P., Jr.; Yilgor, E.; Freelin, R. G. *J. Polym. Sci. A, Polym. Chem.* **1989**, *27*, 3673. (b) Kobayashi, H.; Owen, M. J. *Macromolecules* **1990**, *23*, 4929.

(16) (a) Mukerjee, P. *J. Am. Oil Chem. Soc.* **1982**, *59*, 573. (b) Kunitake, T.; Higoshi, N. *J. Am. Chem. Soc.* **1985**, *107*, 692. (c) Elbert, R.; Folda, T.; Ringsdorf, H. *J. Am. Chem. Soc.* **1984**, *106*, 7687.

(17) Doeff, M. M.; Lindner, E. *Macromolecules* **1989**, *22*, 2951.

(18) Boutin, B.; Youssef, B. *J. Fluorine Chem.* **1987**, *39*, 399.

Table 1. Bulk Characterization Co-hydrosilylated Siloxane Terpolymer PHMS

polymer	MW[a]	C_{ss} (mol %)[b]	C_f (mol %)[c]	N_{ss}[d]	N_f[e]
A	15 150	38	0	29.3	0
B	28 900	64	19	49.3	14.6
C	24 780	21	41	16.2	31.6

[a] MW = average molecular weight of product polymers (calculated on the basis of starting PHMS molecular weight of 4750 and polymer composition assuming that no chain degradation occurs during co-hydrosilylation). [b] C_{ss} (mol %) = disulfide sided chain content in polymer as measured by ^{1}H-NMR. [c] C_f (mol %) = perfluoroalkyl side chain content in polymer as measured by ^{1}H-NMR. [d] N_{ss} = absolute number of disulfide side chains per polysiloxane backbone. [e] N_f = absolute number of perfluoroalkyl side chains per polysiloxane backbone.

at 40 °C for another 12 h. The reaction suspension was then diluted with 20 mL of water, and crude product **5** was extracted with 30 mL of CH_2Cl_2. After the extract was dried over anhydrous $MgSO_4$, methylene chloride was removed at 0 °C under reduced pressure and a colorless liquid was collected. Final distillation of crude product gives a clear liquid of bp 81.5−82.5 (24 mmHg). Yield: 8.98 g (96%). ^{1}H-NMR ($CDCl_3$): δ 3.85 (t, $-OCH_2-$), 4.18 (t, $-CHCH_2O$), 5.34 (m, CH_2═CH), 5.89 (m, CH_2═$CH$$CH_2-$).

Co-hydrosilylation of PHMS with Hydrocarbon/Perfluorocarbon Side Chains (6). To a 8 mL predried glass vial were added 0.114 g (1.89 mmol of Si-H units) of poly(hydrogenmethylsiloxane) (PHMS), 0.30 g (0.87 mmol) of 11-(*n*-pentyldithio)undecyl allyl ether (**4**, see supporting information and ref 12), and 4 mL of anhydrous toluene. After the solution was purged with nitrogen for 3 min, 0.53 g (1.2 mmol) of *n*-pentadecafluorooctyl allyl ether (**5**) and platinum divinyltetramethyldisiloxane−xylene (3%) (catalyst, 3 drops, 0.011 mmol) were added and the mixed solution was stirred at 80 °C for 18 h. Crude polymer product was purified by precipitation−redissolution in methanol/acetone (1:2) and chloroform three times. The purification process was monitored by TLC (chloroform/ethyl acetate, 7:3) until no detectable residual monomer (dithio-containing ether **4**, $R_f = 0.74$) was found in the precipitating solution. Purified polymer **6** was then dried in a nitrogen stream and immediately dissolved in anhydrous chloroform to afford a 3% (by weight) stock solution (stored in the refrigerator) for thin film assembly (after further dilution). Yield: 0.35 g. ^{1}H-NMR ($CDCl_3$): δ 0.075 (br, Si-CH_3), 0.58 (br, Si-CH_2), 0.92 (t, CH_3), 1.30 (br, CH_2), 1.62 (br, S-C-CH_2, O-C-CH_2), 2.70 (t, S-CH_2), 3.35, 3.55, 3.90 (br, br, br, O-CH_2).

Other PHMS polymer-grafted compositions were prepared by the same procedure except that initial PHMS/olefin feed ratios were changed to alter the ratio of grafted alkyl and perfluoroalkyl chains.

Co-hydrosilylation of poly(hydrogenmethylsiloxane) (PHMS) with both dithio- and perfluoroalkyl allyl ethers affords directly the product polymer bearing both pendent fluorocarbon and anchoring disulfide hydrocarbon side chains (Figure 2). Table 1 presents characterization results for the grafted PHMS polymers based on ^{1}H-NMR analysis. Unlike hydrosilylation of PHMS using terminal hydrocarbon olefins directly adjacent to the fluorocarbon chain (e.g., 1*H*,1*H*,2*H*-perfluorodecene), hydrosilylation of the same PHMS by the perfluoroalkyl allyl ether produces the polymer product having the desired perfluoroalkyl side chain attachment features (absence of fluorine transfer from perfluorocarbon α to the terminal olefin).[24] Meanwhile, disulfide species present in the dithioalkyl allyl ether do not cause any significant poisoning of the hydrosilylation catalyst, though a relatively slower reaction compared to conventional hydrosilylation without disulfide moieties is observed.[25] The ^{1}H-NMR spectrum shows that the grafted polymers possess ether-oxygen-adjacent methylene groups derived from both the dithioalkyl allyl ether (δ 3.38) and perfluoroalkyl allyl ether (δ 3.51 and 3.88), illustrating the coexistence of both side chains along the PHMS siloxane backbone.

Polymer Monolayer Film Assembly. Gold substrates for (dithioalkyl)polysiloxane self-assembly were freshly prepared by evaporative deposition of a layer of 1500−2000 Å gold (99.999%, Johnson-Mathey) onto Pd-coated (200 Å) silicon wafer surfaces as described.[12,14] Gold-coated substrates (cut into 3 × 0.8 cm pieces) were immersed into polymer−$CHCl_3$ solutions (0.1−1.5 mM) for up to 72 h, followed by thorough sequential rinsing with $CHCl_3$, EtOH, and Millipore water and drying under pure N_2.

Ellipsometry. Monolayer thicknesses were measured using a Gaertner L117 ellipsometer (70° incident angle, 632.8 nm laser source, three samples, 1−2 spots/sample) by assuming a refractive index of 1.41 for all monolayers (taken by averaging refractive indices for bulk poly[methyl(trifluoropropyl)siloxane] ($n = 1.381$) and poly(methyloctylsiloxane)−poly(hydrogenmethylsiloxane) copolymer (0.54/0.46) ($n = 1.435$)). Arbitrarily changing the n values from 1.35 (highly fluorinated) to 1.47 (primarily hydrocarbon) resulted in less than ±6 Å variation in most calculated monolayer thicknesses.

Contact Angle Analysis. Sessile drop contact angle analysis (Ramé-Hart 100 apparatus) used purified (Millipore 18 MΩ·cm resistivity) water drops (2 μL) on three separate spots on each film surface in a controlled environment (100% RH). Measurements were taken on both sides of water drops at ambient temperature 30−40 s after drops were applied to surfaces. Contact angle data report the average of three drops at different surface locations.

Cyclic Voltammetry. Cyclic voltammograms were measured using an EG&G Model 273 potentiostat/galvanostat and recorded on a Goerz SE790 XY chart recorder. A single compartment, three-electrode glass cell containing a Pt gauze counterelectrode, a calomel (saturated KCl, Radiometer 401) reference electrode (SCE), and a polymer film-coated gold working electrode was used as described previously.[12d] Spin-coated ($CHCl_3$ solution, Headco vacuum chuck, 600−800 rpm) thick polymer films were also prepared. Electrical leads were attached using conducting silver epoxy, and the upper portion of the electrode was masked with Teflon tape,[19] leaving a 0.8 × 0.4 cm^2 electrode area exposed to the solution. Supporting electrolyte was 1 M KCl (99+% EM Science); concentration of the electroactive species ($K_3Fe(CN)_6$ or methylviologen) was 3 mM in Millipore-filtered water purged with argon for 15 min prior to measurement.

Film Thermal Stability. Gold substrates covered with bound polymer monolayer films were immersed in 1,2,3-trichlorobenzene at various elevated temperatures for fixed time periods. At each time point a sample was removed from the solvent, rinsed with chloroform, and dried under N_2. Film was analyzed by aqueous wetting and ellipsometry as described above.

Patterned Monolayer Films. Two types of micropatterned organic thin films of polymers are reported: conventional photolithographic methods fabricated micron-scale gold lines on semiconductor-grade silicon oxide (thermally grown in steam) wafers in a commercial integrated circuit fabrication process in a Class 100 clean room. Additionally, patterns were etched into homogeneous polymer thin films assembled on unpatterned gold surfaces using an automated commercial ion mill (610 Series focused ion beam workstation, FEI Co., Hillsboro, OR). A beam of Ga^+ ions, extracted by field emission from a liquid metal source, accelerated through 25 kV, is passed through focusing lenses and an adjustable aperture and then digitally rastered over a selected target area (see supporting information).

Fourier Transform Infrared Spectroscopy. Bulk transmission and grazing angle spectra were collected on a Nicolet 60SX instrument with a liquid N_2-cooled MCT detector. Grazing angle external reflection spectra used a Spectratech variable angle external reflection accessory (incident angle = 78°, 4 cm^{-1} resolution, 1024 scans). Reference subtraction (fresh, bare gold) and flattening were achieved using Spectracalc software (Galactic Industries), with no curve smoothing or other alterations.

X-ray Photoelectron Spectroscopy. X-ray photoelectron spectroscopy (XPS) experiments were performed on a Surface Science SSX-100 spectrometer (Mountain View, CA) equipped with a monochromatic Al Kα source, hemispherical analyzer, and a multichannel detector. Conditions and methods for these studies were identical to those published previously.[12,14] Loss of fluorine from these samples, resulting from x-ray exposure, was negligible: the fluorine F1s signal varied less than 1% between the start and end of experimental analysis. A Teflon standard was used to calibrate fluorine:carbon ratios. For calculation of XPS elemental composition, the analyzer transmission function was assumed not to vary with photoelectron kinetic energy

(19) Martin, C. R.; Rubenstein, I.; Bard, A. J. *J. Am. Chem. Soc.* **1982**, *104*, 4817.

(KE),[20] the photoelectron escape depth was assumed to vary as $KE^{0.7}$,[20] and Scofield's photoionization cross sections were used.[21]

Angle-dependent XPS data were collected at nominal photoelectron take-off angles of 0°, 55°, and 80°. The take-off angle was defined as the angle between the surface normal and the axis of the analyzer lens system. Using mean free paths calculated from the equations given by Seah and Dench,[22] the sampling depth (three times the mean free path) should decrease from 90 to 15 Å as take-off angle increases from 0° to 80°.

Quadrupole Static Secondary Ion Mass Spectrometry. Static secondary ion mass spectrometry (SIMS) experiments were performed with a Physical Electronics 3700 SIMS system (PHI Electronics, Eden Prairie, MN) mounted on a custom ultra-high-vacuum (UHV) system (see supporting information for details). The ion beam was rastered over a 5 × 5 mm area, and the total exposure time of the sample to the ion beam, including setup and data acquisition, was less than 7 min. Corresponding total ion doses per sample ($<5 \times 10^{12}$ ions/cm^2) are within the generally accepted limit for static SIMS conditions for organic surfaces.[23−25] Both positive and negative secondary ions were collected over a *m/z* range of 0−300 with a nominal mass resolution of unity. Data acquisition and control of the energy filter and quadrupole used the Physical Electronics SIMS software package.

Sample Imaging Using Time-of-Flight Secondary Ion Mass Spectrometry (ToF-SIMS). Imaging of patterned polymer thin films was performed on a Model 7200 Physical Electronics ToF-SIMS instrument (PHI Electronics, Eden Prairie, MN). A gallium liquid metal ion source (LMI Ga), operating at a beam energy of 25 keV, was utilized for all analysis presented in this study (see supporting information for details).

Results and Discussion

Three-component, grafted polysiloxanes bearing both perfluoroalkyl and alkyl disulfide chains were synthesized in various compositions, with three examples shown in Table 1: polymer A bearing only alkyl disulfide chains; polymer B bearing 19 mol % perfluoroalkyl chains and 64 mol % alkyl disulfide side chains; and polymer C bearing 41 mol % perfluoroalkyl and 21 mol % alkyl disulfide side chains.

Polymer Film Thickness and Wettability on Gold Substrates. Perfluoroalkyl and dithioalkyl co-hydrosilylated polysiloxanes were self-adsorbed onto fresh gold-deposited wafers from dilute chloroform solution. Ellipsometric thicknesses of the fabricated polymer films range from 22 to 42 Å (Table 2), consistent with measurements of alkyl disulfide side chain monolayers alone (14 Å),[12] plus the addition of a siloxane layer (4 Å) and a perfluoroalkyl layer (14 Å). Film thicknesses are consistent for each polymer from "batch to batch" after 24 h of dilute solution adsorption (standard deviations of ±4 Å) and do not increase with extended adsorption times up to 1 week, demonstrating only stable monolayer formation and absence of any significant interchain cross-linking by disulfide reduction. Given the uncertainty in the polysiloxane contribution film, thickness differences between films of polymers A and B are not significant. Thicker multilayer films can be prepared from concentrated polymer solutions (20 mM) and extended adsorption times (>72 h). Multilayers presumably result from side chain interlayer associations which increase polymer adsorption and deposition.

Table 2. Polymer Ultrathin Film Properties before and after Treatment at Elevated Temperature in Trichlorobenzene[a]

monolayer film	film thickness (Å)	aqueous contact angle (deg)
octadecanethiol (initially)	23	97
octadecanethiol (after 30 min, 90 °C in solvent)	7	63
polymer A (initially)	22	89
polymer B (initially)	28	92
polymer C (initially)	42	107
polymer C (after 60 min, 90 °C in solvent)	28	107
polymer C (after 120 min, 120 °C in solvent)	18	102
polymer C (after 60 min, 150 °C in solvent)	4	92

[a] Monolayers on gold substrates; solvent = 1,2,3-trichlorobenzene.

The aqueous contact angle shows that the fluorocarbon side chains in the polymers increase film hydrophobicity compared to that of the pure dithioalkyl side chain analog (polymer A) and that surface hydrophobicity increases with increasing the perfluoroalkyl side chain content in the polymer (Table 2). This is attributed to the relative enrichment of fluorocarbon chains in the outermost regions of the monolayer (see XPS film characterization section below). However, compared to other fluorinated surfaces such as Teflon, plasma-deposited perfluoropropane films, and self-assembled monolayers from organic perfluoro compounds,[15,26,27] contact angles for the polymeric monolayers derived from spontaneous adsorption are 7−20° lower, suggesting incomplete coverage of the underlying siloxane backbone and dithio-anchoring side chains by the overlaying perfluoroalkyl chains (Figure 2).

Electrochemical Characterization of Polymer Films on Gold Electrodes. Soluble redox probes, including $Ru(NH_3)_6^{3+/2+}$, $Fe(CN)_6^{3-/4-}$, and methylviologen ($MV^{2+/+/0}$) have often been used for electrochemical measurements on organothiol monolayers in aqueous electrolyte.[28−31] Current attenuation is a function of a number of variables including alkanethiol length, probe chemistry, and film defects (pinholes, grain boundaries). Generally, little Faradaic current is observed through alkanethiol monolayers of dodecanethiol and longer alkyl lengths when assembled on carefully prepared gold substrates.[28]

Cyclic voltammograms for $Fe(CN)_6^{3-}$ on clean, bare gold electrodes show the well-characterized, reversible, one-electron transfer process (data not shown, $\Delta E_p = 60$ mV, $E_{1/2} = 190 \pm 5$ mV).[28−30] Thick, spin-cast films of polymer C (330 Å thick) on gold electrodes are able to completely attenuate electron transfer under the same conditions (not shown). Thinner multilayer films of polymer C on gold electrodes (64 Å) are also very effective at attenuating electron transfer to/from the

(20) Application note from Surface Science Instruments, Mountain View, CA (1987).

(21) Scofield, J. H. *J. Electron Spectrosc. Relat. Phenom.* **1976**, *8*, 129.

(22) Seah, M. P.; Dench, W. A. *Surf. Interface Anal.* **1979**, *1*, 2.

(23) Briggs, D.; Hearn, M. J. *Vacuum* **1986**, *36*, 1005.

(24) We have also studied hydrosilylation of PHMS by (1*H*,1*H*,2*H*-perfluoroalkyl)olefins (C10 and C6) and found in both circumstances an unexpected transfer of fluorine from the $-CF_2-$ group in the α-position to the olefin to the polymer backbone Si atoms. Resultant polymers had less-than-desired side chain density (unpublished result). This undesirable reaction was not observed with compound **5**, where the terminal olefin is moved away from the perfluoroalkyl moieties.

(25) A model study conducted under similar reaction conditions where *n*-pentyl disulfide was used as a "poisoning" additive (replacing dithioalkyl allyl ether) in hydrosilylation of PHMS with 1-octene shows over 90−95% coupling conversion proven by both ^{1}H-NMR and FTIR.

(26) (a) Chau, L.-K.; Porter, M. D. *Chem. Phys. Lett.* **1990**, *167*, 198. (b) Arduengo, A. J.; Moran, J. R.; Rodriguez-Parada, J. R.; Ward, M. D. *J. Am. Chem. Soc.* **1990**, *112*, 6153. (c) Chidsey, C. E. D.; Loiacono, D. *Langmuir* **1990**, *6*, 682. (d) Alves, C. A.; Porter, M. D. *Langmuir* **1993**, *9*, 3507. (e) Lenk, T. J.; Hallmark, V. M.; Hoffmann, C. L.; Rabolt, J. F.; Castner, D. G.; Erdelen, C.; Ringsdorf, H. *Langmuir* **1994**, *10*, 4610.

(27) (a) Haque, Y.; Ratner, B. D. *J. Appl. Polym. Sci.* **1986**, *32*, 4369. (b) Dann, J. R. *J. Colloid Interface Sci.* **1970**, *32*, 302.

(28) (a) Porter, M. D.; Bright, T. B.; Allara, D. L.; Chidsey, C. E. D. *J. Am. Chem. Soc.* **1987** *109*, 3559. (b) Fabinowski, W.; Coyle, L. C.; Weber, B. A.; Granata, R. D.; Castner, D. G.; Sadownik, A.; Regen, S. L. *Langmuir* **1989** *5*, 35.

(29) Nuzzo, R. G.; Dubois, L. H.; Allara, D. L. *J. Am. Chem. Soc.* **1990**, *112*, 558.

(30) Niwa, M.; Mori, T.; Higashi, N. *J. Mater. Chem.* **1992**, *2*, 245; *Macromolecules* **1993**, *26*, 1936.

(31) Chailapakul, O.; Crooks, R. M. *Langmuir* **1993**, *9*, 884.

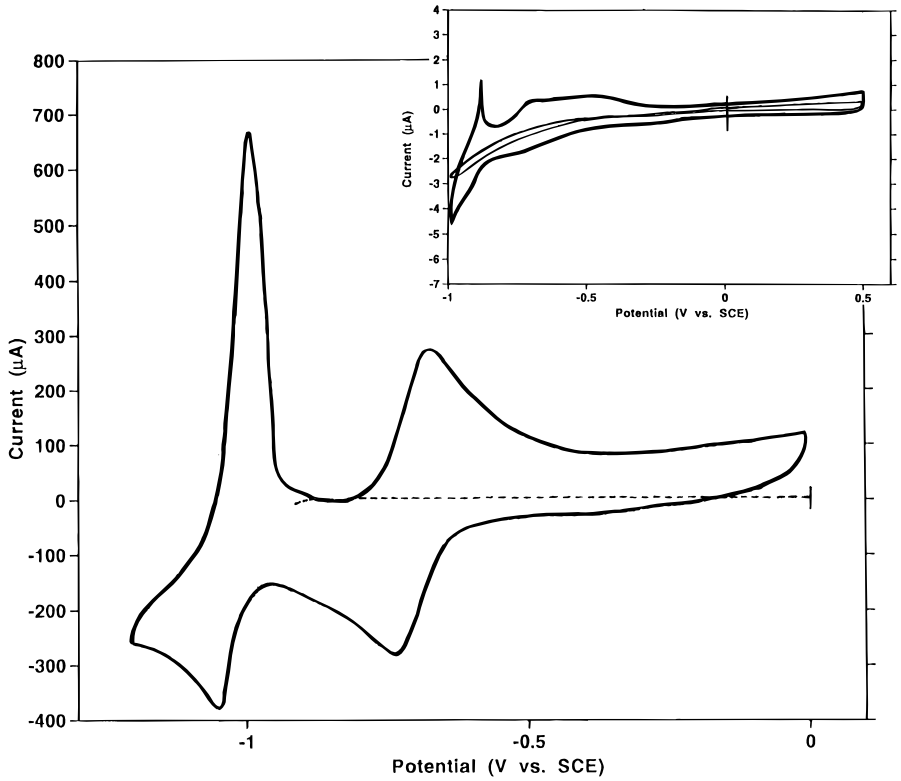

Figure 3. Cyclic voltammograms for MV^{2+} on polymer-coated gold electrodes (probe concentration, 3 mM; scan rate, 200 mV s^{-1}; 1 M KCl supporting electrolyte). Large plot: bare gold electrode (solid line); gold electrode spun-coat (330 Å thick) with polymer C (dashed line). Inset plot: electrode with multilayer film (inner voltammogram) of polymer C (64 Å thick); electrode with monolayer (outer voltammogram) of polymer C (30 Å thick).

redox probe, showing little Faradaic current (data not shown). Monolayer films of polymer C on gold electrodes (30 Å thick) by contrast show a considerably reduced ability to effectively attenuate electron transfer (data not shown), indicating solvent-accessible film defects which permit transport of $Fe(CN)_6^{3-}$ through the polymer barrier to allow electron transfer with the underlying gold electrode.

Because probe chemistry has been implicated in the electron transfer blocking abilities of organothiol monolayers,[31] a methylviologen redox couple was also investigated. The redox properties of viologens in aqueous solutions have been studied extensively.[32−35] Two separate, reversible, one-electron transfer processes are observed for MV^{2+} at −750 and −1000 mV in aqueous solution, with both reduced species, MV^+ and MV^0, retaining water solubility.[36]

Cyclic voltammograms for MV^{2+} on clean, bare gold electrodes show the two characteristic reversible oxidation and reduction waves for this probe (Figure 3, voltammogram A). Again, thick, spin-cast films of polymer C (330 Å thick) completely attentuate electron transfer with this redox couple (Figure 3, voltammogram B). Thinner multilayer films of polymer C (64 Å thick) on gold electrodes are also effective in blocking a substantial amount of Faradaic current as well (Figure 3, voltammogram C). Nevertheless, monolayer assemblies of polymer C on gold electrodes are unable to attenuate electron transfer effectively. The peak-to-peak separation (ΔE) and $E_{1/2}$ values obtained for polymer C monolayer-coated electrodes demonstrate results ($\Delta E = 50$ mV, $E_{1/2} = -750$ mV) identical to those for bare gold electrodes when methylviologen (MV^{2+}) is the redox probe. Despite the fact that peak current (i_p) is reduced by ~80% relative to bare gold, two voltammetric waves (similar to those observed at the bare electrode) are clearly seen at the monolayer-coated electrode. Hence, the voltammetric response of the monolayer-coated film to the MV^{2+} probe is quite different from that of the $Fe(CN)_6^{3-}$ probe. This suggests that the more lipophilic methylviologen penetrates the film more readily than $Fe(CN)_6^{3-}$. Analogous results were observed for monolayers of acrylate polymers on gold.[12d]

Polymer Film Thermal Stability. Film stability differences between monomer and polymer assemblies at elevated temperature in 1,2,4-trichlorobenzene are reflected by temperature-dependent data shown in Table 2. Reductions in aqueous contact angles are correlated to reductions in film thicknesses for all films as a function of solvent temperature, indicating film destruction at elevated temperatures is linked to film stability and film chemistry. Noteworthy are temperature stability differences between monomeric and polymer films. Octadecanethiol films on gold (desorption energy of 35 kcal/mol[37]) are removed within 30 min under these extreme conditions, while polymer films are stable for substantially longer times. This is consistent with previous results reported for polyacrylate-based films on gold. Films of octadecanethiol on gold are readily removed by moderate heating in hexadecane, while dithioalkyl-derivatized polyacrylates are stable over an extended time and elevated temperatures without noticeable effects.[12] Significantly, polyacrylates bearing long alkyl side chains but no sulfur anchoring groups were not able to adsorb to gold to any measurable extent (<5 Å thick), indicating that sulfur-mediated attachment promotes film formation and subsequent stability.[12]

(32) Gomez, M.; Li, J.; Kaifer, A. E. *Langmuir* **1991**, *7*, 1797.
(33) Bae, I. T.; Huang, H.; Yeager, E. B.; Scherson, D. A. *Langmuir* **1991**, *7*, 1558.
(34) Willner, I.; Katz, E.; Riklin, A.; Kasher, R. *J. Am. Chem. Soc.* **1992**, *114*, 10965.
(35) Li, J.; Kaifer, A. E. *Langmuir* **1993**, *9*, 591.
(36) Lei, Y.; Hurst, J. K. *J. Phys. Chem.* **1991**, *95*, 7918.
(37) Nuzzo, R. G.; Fusco, F. A.; Allara, D. L. *J. Am. Chem. Soc.* **1987**, *109*, 2358.

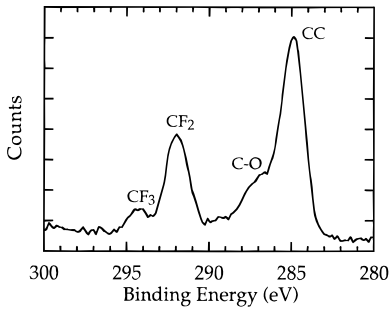

Figure 4. High-resolution XPS Cls spectrum for a polymer ultrathin film of a siloxane terpolymer assembled on a gold substrate. The siloxane terpolymer contained 70% perfluorocarbon and 30% alkyl disulfide side chains.

For polymeric films with disulfide anchoring chains, a time-dependent, thermally enhanced, restructuring phenomenon is plausible, allowing single chemisorbed side chains opportunities to detach but remain surface-localized and to reanchor into ordered side chain clusters while each polymer remains attached to the surface by multiple anchors. Side chain multiplicity promotes film stability and layer permanence while allowing side chain rearrangements toward equilibrium structures. Additionally, the pentanethiol cleavage product from disulfide reduction would likely desorb from the surface under these competitive conditions.[38]

Angular-Dependent X-ray Photoelectron Spectroscopy (ADXPS). Figure 4 shows a typical high-resolution XPS carbon 1s spectrum, detailing the four types of carbon in monolayer films of siloxane terpolymers on gold. The peak centered at 285 eV is characteristic of the hydrocarbon species (e.g., CH_2 present in the alkyl side chains while the peak at 287 eV results from the C−O (ether) carbon present in the side chain linkages.[39] Fluorocarbon species present in the perfluoroalkyl side chains give rise to the peaks at 292 eV (CF_2 groups) and 294 eV (CF_3 groups).[39] Quantitation of high-resolution spectra from the various chemical species in these systems can be compared as a function of take-off angle to yield depth-dependent comparisons of film composition.

Figure 5 presents depth-dependent XPS analyses for monolayer films of four different siloxane polymers on gold. Quantitation for the fluorine:carbon ratio as a function of film depth is collated in Table 3. The most evident point is that all four surfaces have widely different compositions, characteristic of both the differences in bulk side chain stoichiometry and surface enrichment of particular chemical components. The relative abundance of the fluorine signal at all take-off angles changes in direct relation to bulk fluorine content of the samples. Another prominent trend is that as fluorine content increases across the four samples (regardless of sampling depth), carbon signal decreases. The increasing F:C ratio with decreased sampling depth (increased XPS take-off angle) is consistent with the presence of a perfluorocarbon overlayer at the films' outermost surfaces attenuating the carbon signals from film layers underneath. The calculated XPS F:C atomic ratios expected for the polymeric thin films are summarized in Table 4. These values were obtained using the standard expression for calculating XPS intensities and the three layer model depicted in Figure 1 (see ref 40). Mean free paths of 32 and 26 Å were used for the C 1s and F 1s photoelectrons.[22] The composition within each layer was assumed to be homogeneous.

(38) Biebuyk, H. A.; Whitesides, G. M. *Langmuir* **1993**, *9*, 1766.
(39) Dilks, A. In *Electron Spectroscopy: Theory, Techniques and Applications*; Baker, A. O., Brundle, C. R., Eds.; Academic Press: London, 1981; p 277.
(40) Paynter, R. W. *Surf. Interface Anal.* **1981**, *3*, 186.

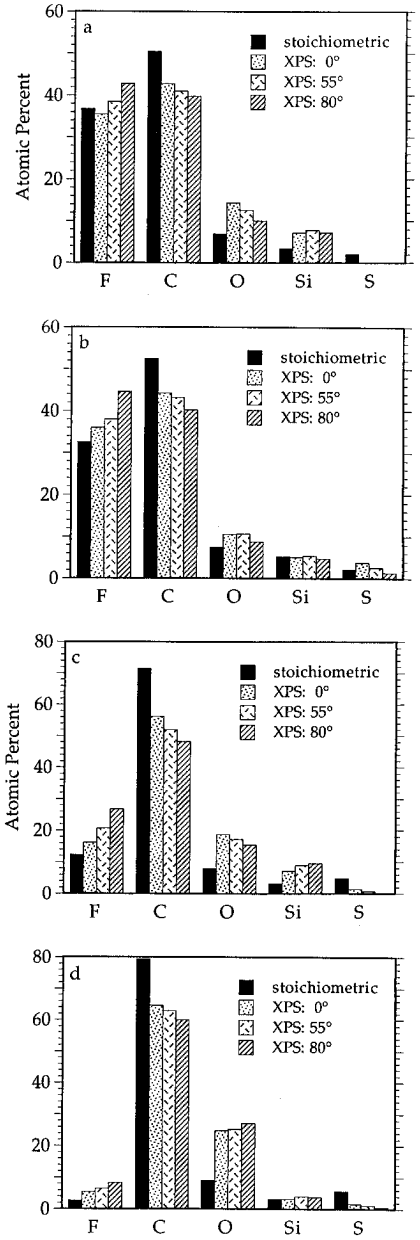

Figure 5. Angular-dependent XPS compositional analysis for polymer ultrathin films of siloxane terpolymers assembled on gold substrates as a function of side chain composition: (a) 70% perfluorocarbon, 30% alkyl disulfide side chains; (b) 41% perfluorocarbon, 21% alkyl disulfide side chains; (c) 23% perfluorocarbon, 77% alkyl disulfide side chains; (d) 5% perfluorocarbon, 95% alkyl disulfide side chains.

The fluorocarbon layer was the outermost layer and assigned a thickness of 14 Å. The siloxane backbone was directly below the fluorocarbon layer and assigned a thickness of 4 Å. The alkyl disulfide layer was the deepest layer and assigned a thickness of 14 Å. The composition of each layer was determined from the stoichiometry of each component (fluorocarbon chains, siloxane backbone, alkyl disulfide chains) and the grafting percentages of the fluorocarbon and alkyl disulfide chains. The calculated values in Table 4 compare favorably with the experimentally determined values in Table 3, considering that quantities such as elastic scattering and surface roughness are not accounted for in the XPS calculations. The main effect of elastic scattering and surface roughness is to increase the relative contribution of deeper layers (e.g., the alkyl disulfide chains) and is the most pronounced at the glancing take-off angle (smallest XPS sampling depth). This probably accounts, at least in part, for the reason the calculated ratios

Table 3. XPS Analysis of Surface Perfluorocarbon Enrichment in Polymeric Perfluorosiloxane Monolayers on Gold[a]

polymer monolayer[b]	fluorine:carbon elemental ratios				
	depth-dependent F:C ratio				F:C ratio (80° take-off angle)
	0° (90 Å)	55° (50 Å)	80° (15 Å)	F:C ratio (stoichiometric bulk)	F:C ratio (stoichiometric bulk)
70%FC/30%SS	0.83	0.94	1.08	0.73	1.5
41%FC/21%SS	0.84	0.91	1.15	0.64	1.8
23%FC/77%SS	0.29	0.40	0.56	0.17	3.3
5%FC/95%SS	0.09	0.10	0.14	0.03	4.7

[a] XPS 0°, 55°, and 80° take-off angles represent XPS sampling depths from 90 Å (deep) to 15 Å (shallow). [b] FC represents perfluoroalkyl graft; SS represents alkyl disulfide graft.

Table 4. Calculated XPS F:C Atomic Ratios for Perfluorosiloxane Monolayers[a]

polymer monolayer	calcd F:C atomic ratio		
	0°	55°	80°
70%FC/30%SS	0.72	0.82	1.13
41%FC/21%SS	0.60	0.69	1.06
23%FC/77%SS	0.21	0.28	0.81
5%FC/95%SS	0.04	0.06	0.32

[a] Based on ref 40.

show a larger increase in the F:C ratio from 0 to 80° take-off angles than the experimental ratios do.

Data from Table 3 show that relative perfluorocarbon enrichment (compare 80° take-off angle data against stoichiometric bulk data) is significantly larger for samples with lower bulk perfluorocarbon content. As perfluorocarbon content in the polymer increases, relative surface enrichment decreases. Additionally, as a function of increasing take-off angle (decreasing depth) for each sample, fluorine signal increases beyond the stoichiometric bulk content, further supporting the presence of an enriched perfluorocarbon overlayer in these polymer monolayer films. This is paralleled by the predicted opposite trend in carbon signal with take-off angle; that is, a consistent decrease in carbon below its bulk content with increasing take-off angle (decreasing depth).

Sulfur content steadily decreases in all film surfaces with decreasing sampling depth, reaching concentrations significantly below the stoichiometric bulk content at the shallowest sampling depth. This observation is consistent with the sulfur anchor groups located under the film adjacent to the gold interface. Furthermore, the silicon signal remains roughly constant despite the various changes in other species with sampling depth, indicating a relatively diffuse partitioning of the polysiloxane backbone between a perfluorinated overlayer and an alkyl disulfide underlayer. Some samples show a clear maximum in the silicon signal at intermediate depths, consistent with a polysiloxane-enriched layer between two adjacent, compositionally distinct zones. The ratios of fluorine:silicon, carbon:silicon, and sulfer:silicon are further evidence for a layered polymer monolayer structure: perfluoroalkyl-enriched outer surface layer, siloxane-enriched intermediate stratum, and a basal, anchoring layer containing sulfur (disulfide) anchoring chains.

Static Secondary Ion Mass Spectrometry (SIMS). A significant amount of recent work characterizing self-assembled organic films has used SIMS surface analysis.[41] Static SIMS measurements complement XPS data by virtue of the high surface sensitivity of static SIMS (~20 Å) which allows a more complete examination of chemistry at the outermost film surface. ADXPS measurements support a stratified monolayer assembly

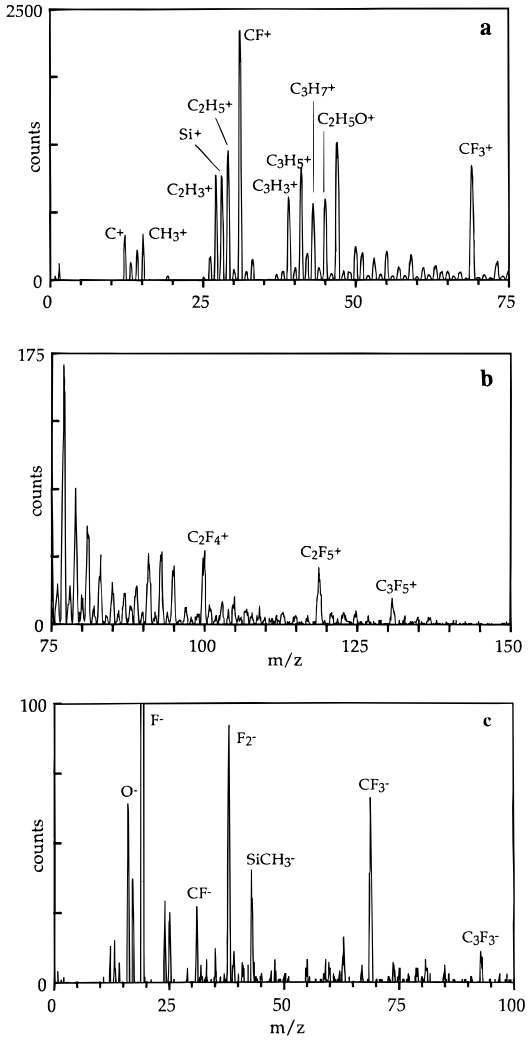

Figure 6. Statis SIMS results for a monolayer film of polymer B on gold: (a) positive ion spectrum (m/z = 0 to 75); (b) positive ion spectrum (m/z = 75 to 150); (c) negative ion spectrum (F^- counts = 1900).

enriched by perfluorocarbon chains at its outer surface (Figure 5, A−D). Static SIMS results for the terpolymer monolayer film of polymer B on Au, shown in Figure 6, provide yet further support for this model. Prominent positive ion peaks (Figure 6a) are observed for fragments at m/z = 31, 69, 100, 119, and 131, corresponding to perfluoroalkyl fragments.[42] Peaks representing positive ion fragments of the allyl ether chain terminus linking the perfluoroalkyl and disulfide side chains to the siloxane backbone are observed at m/z = 27, 29, 39, 41, 43, and 45. The peak at m/z = 28 can be attributed to Si^+ from the siloxane backbone. The negative secondary ion spectrum (Figure 6b) also exhibits prominent peaks corresponding to

(41) (a) Huang, J.; Hemminger, J. C. *J. Am. Chem. Soc.* **1993**, *115*, 3342. (b) Frisbie, C. D.; Martin, J. R.; Duff, R. R.; Wrighton, M. S. *J. Am. Chem. Soc.* **1992**, *114*, 7142. (c) Tarlov, M. J.; Burgess, D. R. F.; Gillen, G. *J. Am. Chem. Soc.* **1993**, *115*, 5305.

(42) Castner, D. G.; Lewis, K. B.; Fischer, D. A.; Ratner, B. D.; Gland, J. L. *Langmuir* **1993**, *9*, 537.

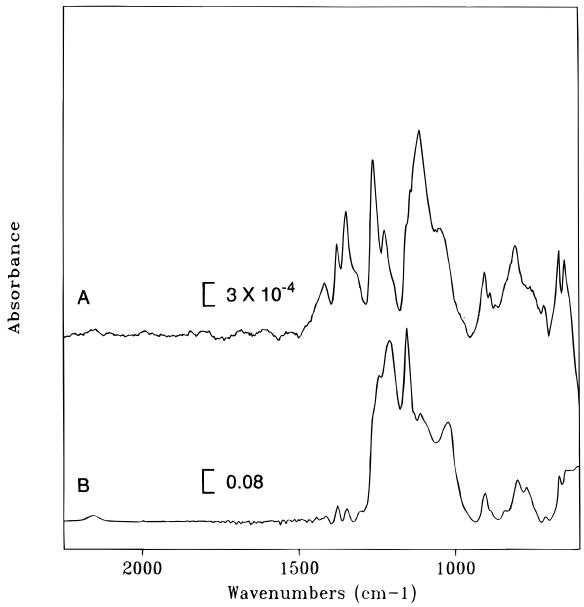

Figure 7. FTIR spectra for a polysiloxane derivatized with 74% perfluoroalkyl side chains and 19% dithioalkyl side chains: (A) grazing incidence reflection spectra (78°, $E_\perp$) for a monolayer assembled on gold and (B) bulk transmission spectra. Scale bars indicate respective absorbance units for each spectra.

perfluoroalkyl fragments (m/z = 19, 31, 38, 69, 93, etc.) and peaks corresponding to fragments from the siloxane backbone (m/z = 16 and 43). Most importantly, the intensity of negative ions originating from the sulfur anchor groups (S^- and SH^- at m/z = 32 and 33) are very weak. In contrast, assembled monolayers of siloxane oligomers[14] that have a nearly homogeneous distribution of thiol groups throughout the film produce very strong S^- and SH^- signals.[43] Thus, the prominent perfluoroalkyl fragments and very weak sulfur fragments of Figure 6 are consistent with the stratified monolayer assembly depicted in Figures 1 and 2.

Infrared Spectroscopy. Comparisons of vibrational FTIR spectra acquired from these same ultrathin polymer films at grazing incidence vs bulk coated polymer films also support film organization through differences regarding both vibrational peak position and relative intensity.[44,26e] Figure 7 presents the FTIR spectral region with various C−F-active IR bands for a perfluoroalkyl-grafted polysiloxane monolayer on gold containing 74% grafted perfluoroalkyl chains. The transmission spectra of the bulk perfluoroalkyl-grafted polysiloxane film (Figure 7B) is nearly identical to that calculated for a randomly oriented perfluoroalkyl system.[26d] Bands at 1373 and 1344 cm^{-1} represent the symmetric CF_2 stretch progression, or what has been recently called the "axial CF_2 stretching vibrations."[26e] Bands at 1236, 1205 and 1151 cm^{-1} represent fluorocarbon asymmetric stretches [$\nu_a(CF_2)$]. Other bands characteristic of the polysiloxane backbone [e.g., ν(Si−O), 1105 cm^{-1}] and various hydrocarbon assignments are also present, but the dichroism of the bands representing fluorocarbon-grafted side chains, in particular, are important in understanding monolayer organization.

The upper spectrum (A) in Figure 7 was recorded at a grazing incidence (78°, $E_\perp$) for a monolayer of the same polysiloxane (74% perfluoroalkyl side chain content) on gold. Dramatic changes in this spectra compared to the bulk spectra (B) as well as polarization effects reflected in grazing incidence spectra are indicative of structure in the polymeric monolayer. So-called "axial CF_2" bands at 1373 and 1346 cm^{-1} and the 1257 cm^{-1} band have substantially increased intensity in the reflection spectrum (Figure 7A) compared to the bulk spectrum (Figure 7B). Recently, Lenk et al. have interpreted this effect to be due to alignment of the axial CF_2 stretch dipole moment change along helical $-CF_2-$ chains parallel with the surface normal.[26e] Enhancement of the 1257 cm^{-1} band in (Figure 7A), tentatively assigned to ν(C−C) and δ(C−C−C) components,[26e] also supports orientation of perfluoroalkyl groups normal to the surface. Additionally, changes of relative intensities for axial CF_2 stretching bands at 1373 and 1346 cm^{-1} in grazing angle spectra are consistent with spectra for well-ordered monolayer films of perfluoroalkanethiols on gold.[26] In fact, reversal of these intensity ratios between bulk (Figure 7B) and reflection (Figure 7A) spectra is consistent with a randomly ordered to organized transition.[26c]

Lastly, asymmetric CF_2 stretching bands at 1221, 1205, and 1151 cm^{-1} decrease their relative intensity in the grazing angle reflection spectrum compared to bulk. This, again, is consistent with attenuated monolayer vibrations from dipole moment changes perpendicular to a perfluorocarbon helical axis oriented *normal* to the surface. A band observed at 725 cm^{-1}, unique to the reflection spectra and characteristic of the CF_3 end group stretching vibration, would be expected to be intensified in the grazing angle spectrum for chains oriented normal to the surface.[26d] This generates an overall orientation of the C−F bond in each CF_3 group relatively perpendicular to the substrate surface.[45] Polysiloxanes with varied perfluoroalkyl contents all exhibit these spectral features (data not shown). Changes in the FTIR vibrational modes in the reflection spectra of the polymer monolayers compared to their bulk transmission spectra support a structural model where polymer fluorocarbon side chain packing in the ultrathin films is more organized anisotropically toward the surface normal than that in bulk coatings.[26,45]

Polymer Film Structure. On the basis of this extensive set of surface analytical data, the structural picture supported by FTIR, XPS, and SIMS data on these monolayer films is one where perfluoroalkyl side chains extend away from the substrate-anchored siloxane backbone to enrich the outermost film region in an orientation more vertical than horizontal to the substrate plane. Such an approximation is, in fact, quite close to the structure proposed in Figure 1 for these ultrathin films. The only specific chemical interactions mediating this organization are the gold−thiolate bonds formed by anchoring side chains. This ensures that some fraction of the alkyl disulfide grafted chains are directly adjacent to the gold surface. Intrinsic immiscibility (unfavorable enthalpy of mixing) between this anchored alkyl component and more mobile siloxane and perfluoroalkyl substituents likely promotes formation of a stratified organic film, rich in perfluorinated groups near its surface. However, an alternative explanation is that specific alkyl side chain attachment to gold excludes the rest of the polymer from this interface from entropic reasons, promoting perfluoroalkyl surface enrichment as a consequence of polymer interface exclusion. It is not unreasonable to assume some degree of surface perfluoroalkyl self-association to form an incomplete yet significantly organized overlayer atop the polysiloxane superstructure: several precedents for such self-organization in perfluoroalkane systems have been reported.[46]

(43) Castner, D. G.; Grainger, D. W. Unpublished results.
(44) Sun, F.; Mao, G.; Grainger, D. W.; Castner, D. G. *Thin Solid Films* **1994**, *242*, 106.
(45) Bertilsson, L.; Liedberg, B. *Langmuir* **1993**, *9*, 141.
(46) (a) Russell, T. P.; Rabolt, J. F.; Twieg, R. J.; Siemens, R. L.; Farmer, B. L. *Macromolecules* **1986**, *19*, 1135. (b) Mahler, W.; Guillon, D.; Skoulios, A. *Mol. Cryst. Liq. Cryst., Lett. Sect.* **1985**, *2*, 111.

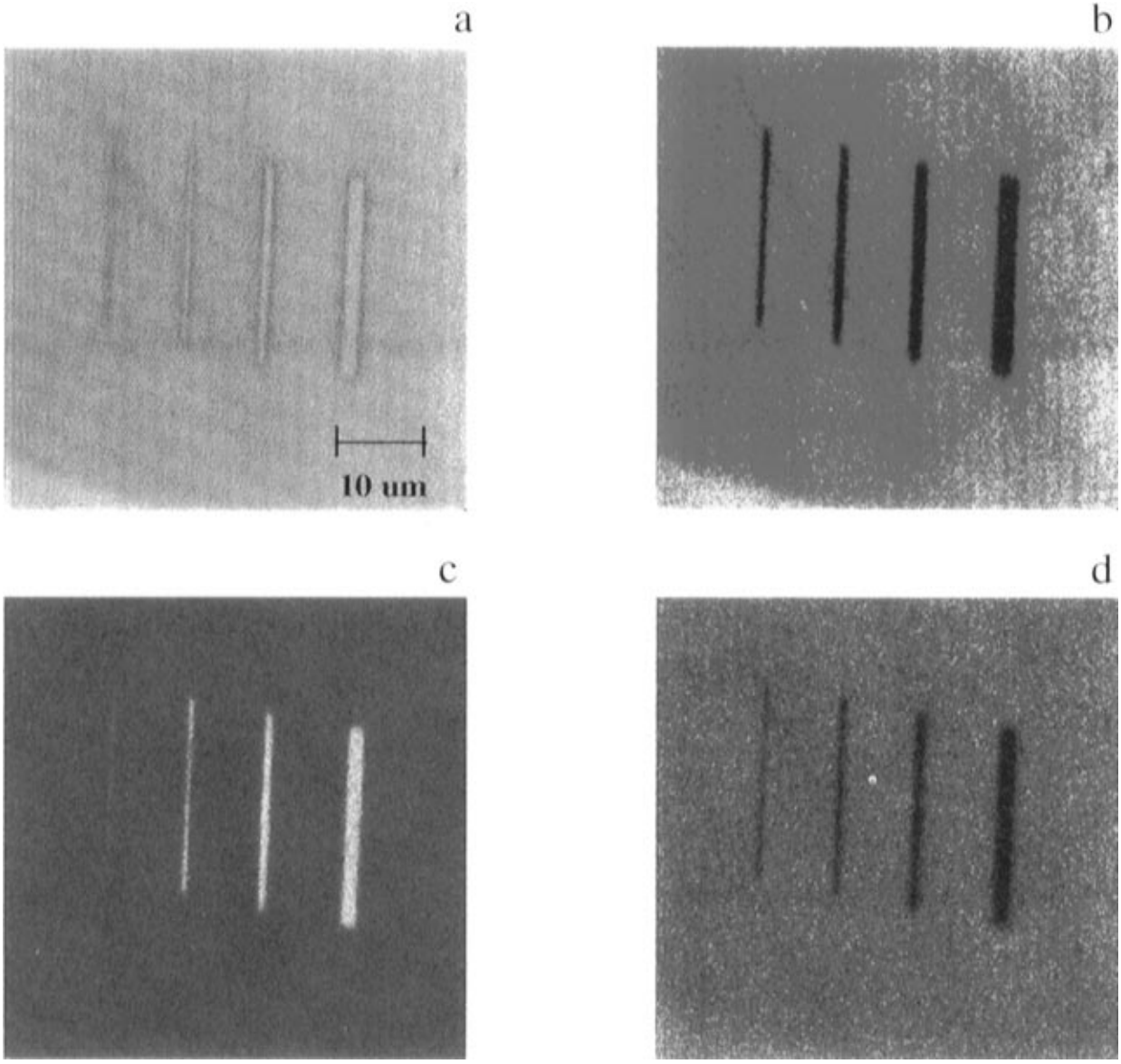

Figure 8. ToF-SIMS imaging results for polymer ultrathin films of siloxane terpolymers lithographed after assembly using ion milling: (a) total ion yield; (b) fluorine ion yield; (c) CN^- contaminant ion yield exposed in gold substrate after ion milling; (d) Au substrate ion yield.

Surface Imaging Using Time-of-Flight Secondary Ion Mass Spectrometry (ToF-SIMS). Time-of-flight mass spectrometry (ToF-SIMS) provides yet again a further dimension to the surface analysis of these films by yielding both high mass resolution for surface-derived fragments as well as the capability to conveniently map and image all possible film chemical fragment combinations across the sample's surface. Several recent studies of organic thin films have used ToF-SIMS to image patterned substrates.[47] Spectroscopy and imaging were performed on patterned polymer films in both positive and negative SIMS modes by ToF-SIMS. Quasi-molecular ions (monomer units) were not observed in any of the acquired spectra from the perfluorinated polymers; however, characteristic fragment ions were observed. In the positive SIMS spectrum the base peak was CF (*m/z* 31). Many fragment ions associated with the fluorinated chain were observed such as CF, CF_2, CF_3, C_3F_3, C_2F_4, and C_3F_5. In addition, fragment positive ions originating from the siloxane portion of the polymer were also observed; Si, CH_3Si, and SiC_3H_9. In negative SIMS, fluorine was the base peak in the spectrum and, again, fragment ions originating from the perfluoro alkyl chains (e.g., CF, CF_3, C_2F_2, C_3F_3, C_2F_5, C_3F_5...) are observed (data not shown).

Figure 8 is a ToF-SIMS image acquired from a 50 × 50 μm area (256 × 256 pixels) of ion-milled lines (20 μm long and widths ranging from 2 to 0.2 μm) in homogeneous polymer assemblies. The upper left quadrant (Figure 8a) shows the total secondary ion image. The contrast in the total ion image is the result of variation in the secondary ion yields for the species present in the analysis area. For this sample, topography (i.e., shadowing of the primary ion beam) does not contribute to the observed contrast as the etching process removes monolayers of material. The upper right quadrant (Figure 8b) shows the fluorine (F^-) distribution and hence the distribution of the perfluorosiloxane. Images may be generated from any of the fluoro-containing fragments; however, the fluorine (F^-) image provides the highest S/N ratio (image quality) from which line scans can easily be determined. The line scans generated from this image (data not included) show that actual line widths from the ion mill etched areas are 1.3, 2.1, 2.5, and 3.5 μm, respectively, which deviate substantially from the ion beam's focused resolution during milling. The lower left quadrant (Figure 8c) shows the distribution of CN^- ion, likely a trace-

(47) (a) Offord, D. A.; John, C. A.; Griffin, J. H. *Langmuir* **1994**, *10*, 761. (b) Vargo, T. G.; Thompson, P. M.; Gerenser, L. J.; Valentini, R. F.; Aebischer, P.; Hook, D. J.; Gardella, J. A. *Langmuir* **1992**, *8*, 130.

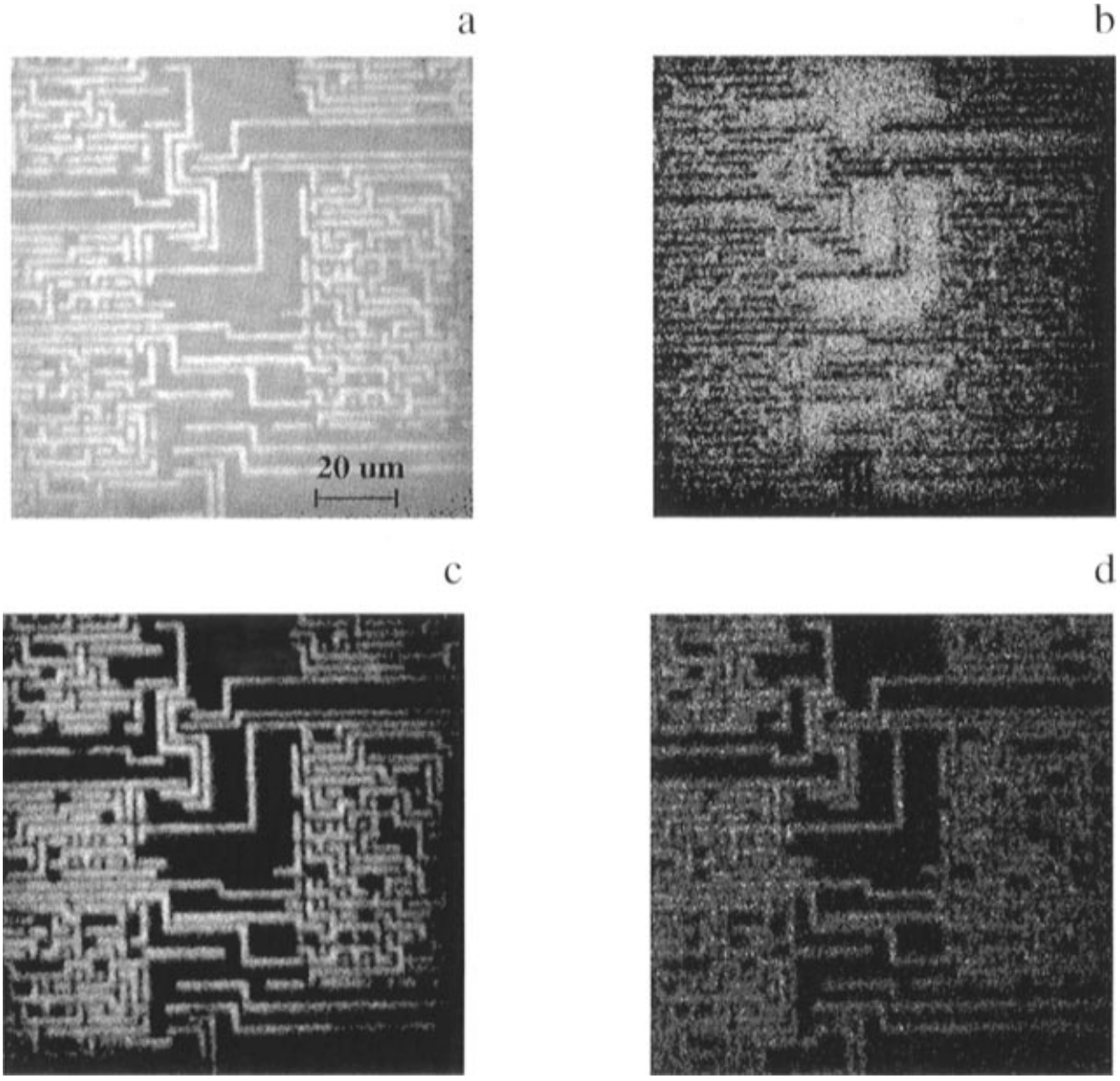

Figure 9. ToF-SIMS imaging results for siloxane terpolymers assembled from dilute solution onto photolithographed gold lines on SiO_2 wafers: (a) total ion yield; (b) oxygen ion yield (primarily SiO_2 substrate); (c) perfluorocarbon fragment ion yield (polymer film); (d) Au ion yield (lithographed gold lines).

level contaminant in the gold underlayer, which even at a gold purity of 99.999% seems exposed during the ion milling of the organic overlayer. This ion is not detected by XPS but is easily imaged by the ToF instrument in the ion-milled, exposed gold areas. Detecting and locating contaminants in these materials is very important to the understanding and characterization of these materials. The parallel analytical capabilities of both XPS and ToF-SIMS is, therefore, significant and complimentary.

Figure 9 shows analogous ToF-SIMS images for bound polymer films of the siloxane terpolymer C anchored specifically on photolithographed gold lines (2 μm wide) on SiO_2 wafers. We have previously used scanning Auger mapping to demonstrate that disulfide-derivatized acrylate polymers attach to lithographed gold lines specifically by solution exposure of patterned wafers to soluble polymer.[12c] The ToF-SIMS ion fragment "maps" show that the siloxane terpolymer attaches exclusively to the patterned gold lines, mediated by Au substrate−disulfide side chain anchor interactions. Oxygen negative ions (Figure 9b) map to SiO_2 areas while CF^- ions (Figure 9c) map accurately to the gold lines (compare to Figure 9d). Both sets of ToF-SIMS images provide detailed spatial information on the distribution of surface chemistry present in thin polymeric film. The high mass resolution spectra accompanying these ion fragment maps will be discussed in a future publication.

Conclusions

Our interpretation of these data confirms our hypothesis that polymer coil-to-monolayer transitions can be driven by specific anchoring events at interfaces, and together with chain−chain immiscibility, allowing three-dimensional polymer coils in solution to form two-dimensional networks at the expense of entropic tendencies. Significantly, poorly miscible components mutually tied to a common polymer main chain are compelled to segregate, even in these two-dimensional monolayer film assemblies. Low surface energy perfluoro side chains, therefore, migrate to the surface of these films, away from anchoring hydrocarbon chains, yielding a distinctly structured, self-organized polymer monolayer with a fluoroalkyl-enriched surface.

Dense, monolayer polymer films can be anchored on solid surfaces by spontaneous assembly from dilute solution. Judicious choice of polymer components leads to films which self-

organize to yield bound anisotropic structures. We have also demonstrated selected partitioning of polymer components to yield surface enrichment. This has practical implications, namely, tailoring of interfacial properties by predictable anchoring of polymers to surfaces in ultrathin arrays, and further routes for chemically modifying these arrays *in situ* as a versatile surface modification strategy. These methods may also prove useful for fundamental studies of polymer chain behavior at interfaces.

Acknowledgment. We thank C. R. Martin, M. D. Porter, J. D. Andrade, H. Wolf, J. Venzmer, M. Lerner, and T. J. Lenk for their critique and suggestions. The authors also thank Dr. Bob Drosd (BIT, Inc., Portland, OR) for supplying freshly photolithographed gold lines on silicon wafers and Dr. J. K. Hurst (Washington State University) for assistance with cyclic voltammetry experiments. John Hunt and Jim Cser (Oregon Graduate Institute) provided outstanding assistance with focused ion beam milling to prepare lithographed polymer surfaces. Support is gratefully acknowledged from the Whitaker Foundation (D.W.G.), National Science Foundation/EPRI Grant MSS-9212496 (D.W.G.), National Science Foundation Grant DMR-9357439 (D.W.G.), Tektronix, Inc. (D.W.G.), and National Institutes of Health Grant RR-01296 (D.G.C.).

Supporting Information Available: Text giving experimental details (3 pages). This material is contained in many libraries on microfiche, immediately follows this article in the microfilm version of the journal, can be ordered from the ACS, and can be downloaded from the Internet; see any current masthead page for ordering information and Internet access instructions.

JA952225T